SUPPLEMENT TO THE *WELDING JOURNAL*, JULY 2009
Sponsored by the American Welding Society and the Welding Research Council

Error Analysis of a Three-Dimensional GTA Weld Pool Surface Measurement System

The proposed system, which uses specular reflection of the pool surface as a means of measurement, was shown to be accurate

BY H. SONG AND Y. M. ZHANG

ABSTRACT

Measurement of weld pool surface is an important research area in the welding community. In recent years, many vision-based approaches have been proposed that have achieved certain successes in this area. However, the accuracy of the measurement results in these systems deserves further consideration since the shape information of small weld pool surface may be used to validate welding models and control the process. In this paper, specific error analysis is given for our early proposed three-dimensional gas tungsten arc (GTA) weld pool surface measurement system, which utilizes the specular reflection characteristic of pool surface to do the measurement. First, all the measurement procedures related to the system error were introduced. Then the included error sources in each procedure were analyzed. Last, experiments and simulations were conducted to estimate measurement system error and other errors quantitatively. Through error analysis, the accuracy of the proposed measurement system was validated and the main error source was identified. This work is not only useful to improve the accuracy of our measurement method, but also instructive for error analysis of the others.

Introduction

The welding process has been widely applied in many manufacturing industries. Since welding is a labor-intensive and skill-required operation, automation of the process becomes an attractive way to improve its productivity and quality. Although current welding robots can provide consistent motion, they lack the intelligence that skilled human welders possess to achieve good weld quality by observing the weld pool (surface). Moreover, measurement of the weld pool surface can provide critical experimental data for weld pool modeling research. Hence, precise measurement of the weld pool surface becomes a fundamental requirement for both automated welding machines and welding researchers. In recent years, a few techniques have been applied to sense the weld pool, such as machine vision, X-ray radiation, ultrasonic and acoustic emission, etc. (Refs. 1–4). Among the existing methods, vision-based sensors have been studied the most extensively. In these systems, vision-based sensors are used to acquire images of the weld pool surface, and image processing is followed to extract weld pool surface size/shape information so that control algorithms can use it as a feedback to adjust welding processes (Refs. 5–7).

One early experiment based on direct view of the weld pool has been done in the Welding Research Laboratory at the University of Kentucky by using a specially designed commercial camera whose high-speed shutter was synchronized with a short duration pulsed illumination laser (Ref. 5). This camera allowed the bright arc light to be eliminated from the image by the intense laser light, and the two-dimensional (2-D) boundary of the weld pool was clearly imaged, as shown in Fig. 1A. Obviously, the accuracy of this 2-D measurement system depends on the proposed 2-D weld pool model and the image processing result (Ref. 5). To use this system in three-dimensional (3-D) weld pool surface imaging, the illumination laser is projected through a frosted glass to form multiple strips. An image with 3-D information can thus be acquired, as shown in Fig. 1B (Ref. 6). Due to the difficulty of precise system positioning, the system is only used for 3-D observation not 3-D measurement. The camera used in the above approaches is extremely expensive and the frame rate can only reach 30 frames per second due to the use of the high-power pulsed illumination laser.

In another system, a structured light technique has been applied to acquire the profile of the weld pool surface by Saeed (Ref. 4). In his system, a laser line is projected onto the center of the weld pool surface, and it is observed by a compact camera system fitted with a band-pass filter. One example of the captured images is shown in Fig. 1C. The 3-D shape of a weld pool profile can be seen. However, the interference of a strong weld arc degrades the quality of the image. The error in this measurement system is in an acceptable range (Ref. 4). In a separate effort, Mnich and his colleagues used a stereovision method to determine the three-dimensional shape of the weld pool (Ref. 7). The main error in this system comes from the correspondence process. Another approach used a similar principle but introduced the biprism technique to reduce the number of needed cameras from two to one (Ref. 8). The accuracy of this system as mentioned by the authors is reasonable. In another sensing system developed by

KEYWORDS

Weld Pool Surface
Specular Reflection
3-D Reconstruction
Error Analysis
Gas Tungsten Arc Welding
GTAW

H. SONG and Y. M. ZHANG (ymzhang@enrg.uky.edu) *are with Center for Manufacturing and Department of Electrical and Computer Engineering, University of Kentucky, Lexington, Ky.*

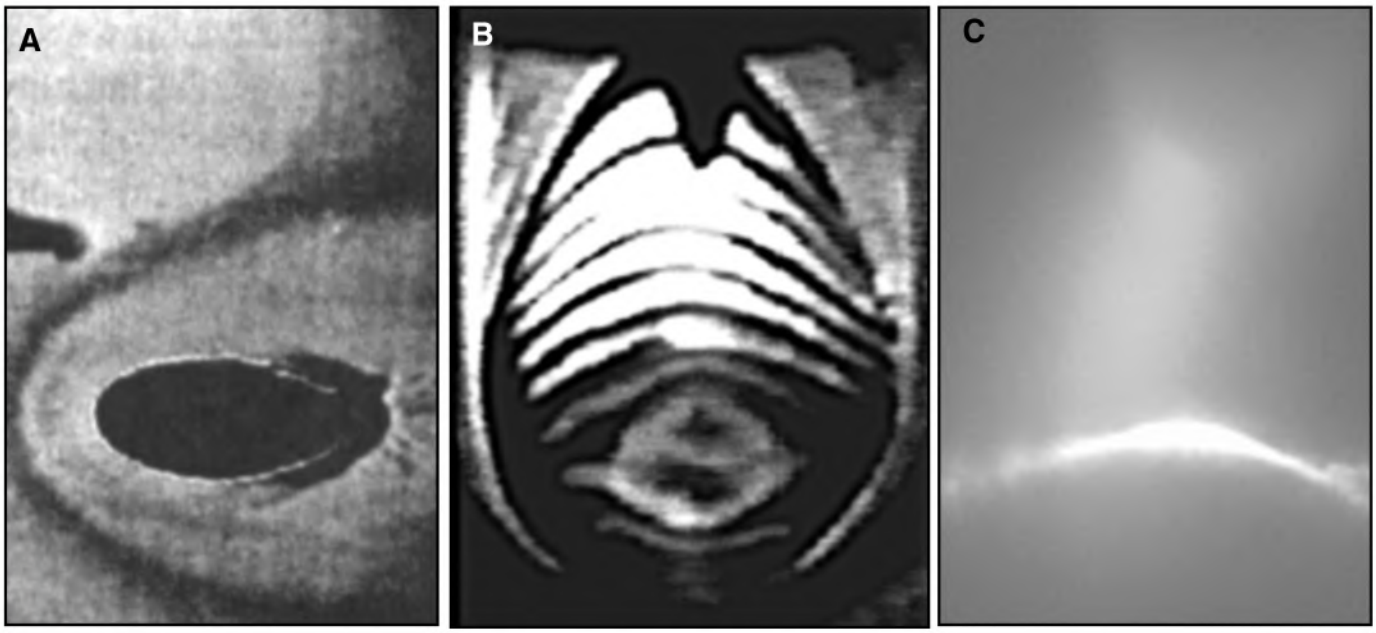

Fig. 1 — Captured images for weld pool surface measurement. A — 2-D shape (Ref. 5); B — 3-D shape (Ref. 6); C — depth/profile extraction (Ref. 4).

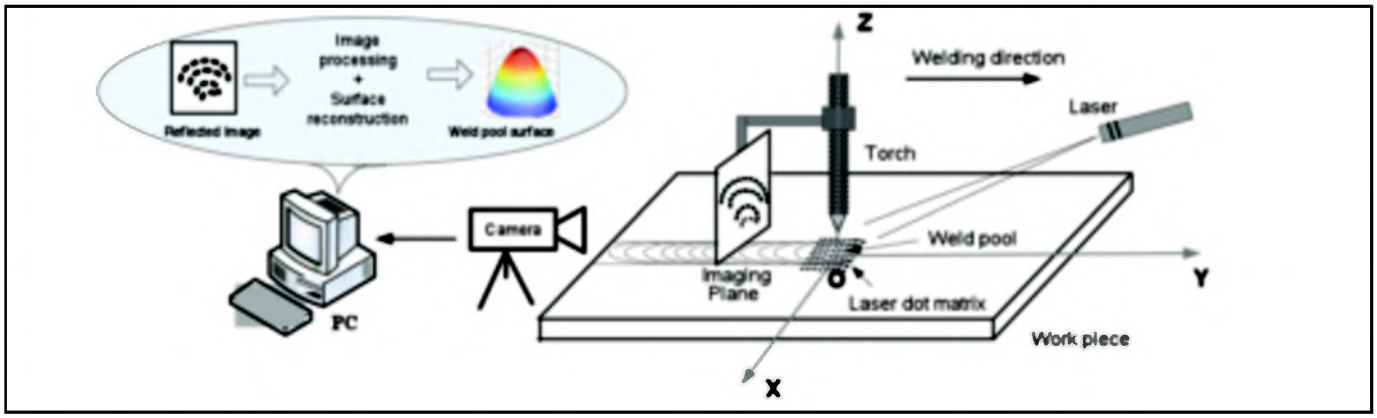

Fig. 2 — Diagram of the proposed measurement system.

Zhang et al. (Ref. 9), the 3-D shape of the weld pool is reconstructed from a 2-D image of the pulsed gas metal arc welding (GMAW-P) process based on the proposed mathematic model. The assumed model may affect the accuracy of the measurement. As another indirect method, the shape-from-shading (SFS) technique was introduced to reconstruct the 3-D weld pool surface by Zhao (Ref. 10). Shape-from-shading is a technique of recovering 3-D information from the variation of shading on the image. Li and Du, respectively, have done further research in this area and greatly improved the methods (Refs. 11, 12). Their approaches all performed good results. However, there are still a lot of difficulties in using the SFS technique, such as the interference of strong arc light. As can be seen, while all these methods have achieved certain successes, more accurate and cost-effective methods are still needed.

In our previous work, a different approach was proposed to observe the 3-D gas tungsten arc (GTA) weld pool surface (Refs. 13–16). Because of the simplicity (simple system structure and procedures), practicality (practical components, such as 20-mW low-power laser diode), and efficiency (high-contract and simple acquired images) of the proposed method, it is more suitable for manufacturing process. Furthermore, the system can be more compact if the imaging system is replaced by an image sensor chip with a band-pass filter (Ref. 13). The accuracy of the reconstruction results is discussed qualitatively, but not quantitatively.

In this paper, an extensive error analysis is conducted for the proposed 3-D measurement system. First, the procedures in the system and the related error sources are introduced. Then these errors are classified and the measurability of the errors is discussed. Following that discussion, the overall measurement system error and the other kinds of errors are further investigated either by experiments or by simulations. At last, the findings are addressed.

Review of Measurement System

System Structure

It can be seen in some previous studies (Refs. 4, 5) that specular reflection takes place on the molten weld pool surface when laser light is projected onto it. In order to take advantage of the pool surface's reflection property, a new 3-D GTA weld pool surface measurement system is proposed (Refs. 13–16). Its diagram is shown in Fig. 2. In this system, a dot-matrix structured laser pattern is projected onto the weld pool surface at a certain angle, and an imaging plane is placed on the other side to intercept its reflection from the pool surface. Meanwhile, a high-speed camera fitted with a band-pass filter (centered at laser wavelength) is used to capture the reflected images on the imaging plane. The captured

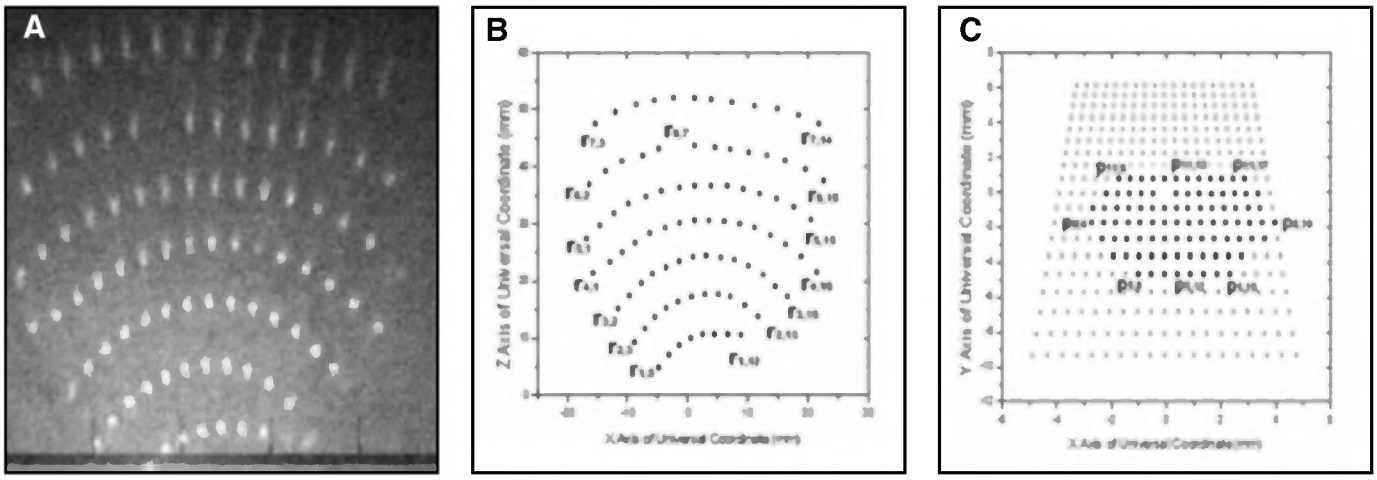

Fig. 3 — Reflected image processing results. A — Acquired reflected image; B — extracted reflected dots $r_{i,j}$ on imaging plane (row number i, column number j) (Ref. 16); C — corresponding projected dots $p_{i,j}$ on workpiece (row number i, column number j) (Ref. 16).

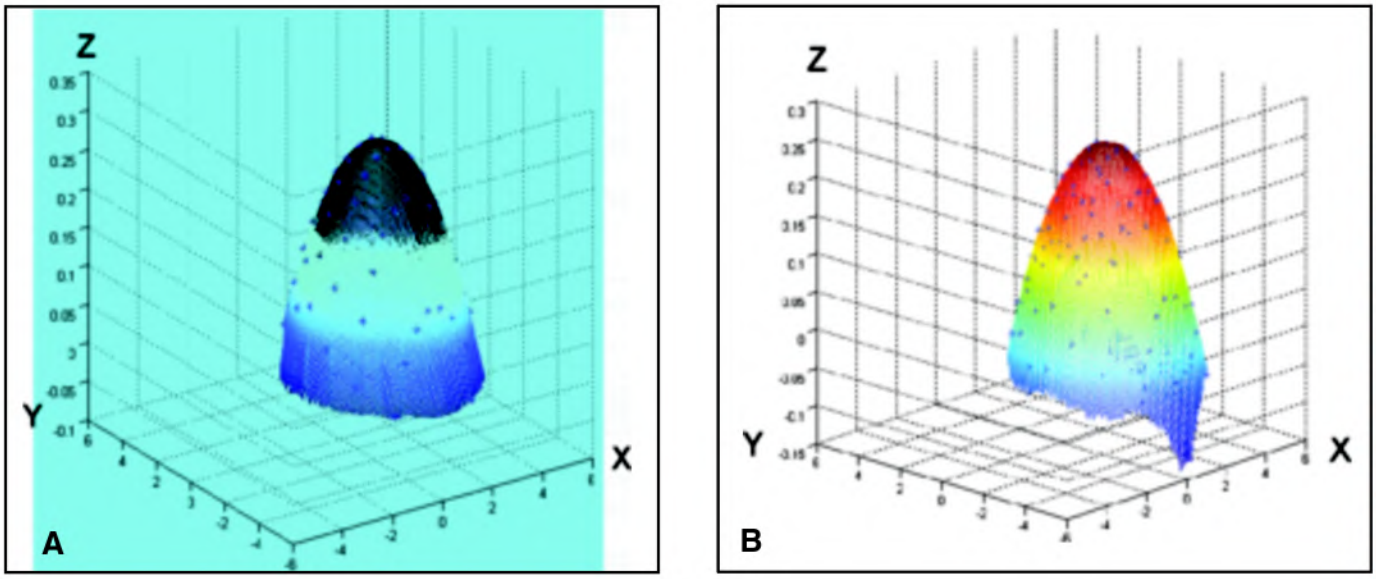

Fig. 4 — Results of different reconstruction schemes (Ref. 16). A — IRS; B — ERS.

images are then processed using developed image processing algorithms and surface reconstruction schemes. Thus 3-D shape of weld pool surface can be reconstructed. In the following, the design and measurement steps along with the introduced errors are briefly introduced and more detailed descriptions can be found in our early work (Refs. 13–16).

Component Selection

Laser (Pattern)

Through investigation, a commercially available 685-nm low-power continuous laser diode (20-mW StockerYale's Lasiris™ SNF) and a diffractive lens with 19 × 19 dot-matrix structured light pattern were selected (Ref. 14). Theoretically, the higher power and the denser pattern can produce higher contrast in the reflected image and provide more accurate information for weld pool surface measurement.

Imaging Plane

In the designed system, an imaging plane is used to intercept the reflected laser pattern for image acquisition. To ensure the visibility of the reflected pattern, a piece of 4 × 4 in. thin glass attached with a sheet of paper was used as the imaging plane. The glass can help resist the high temperature of the arc, but at the same time it may changes the route of the reflected lights.

Camera

Considering the dynamic characteristic of the weld pool, an OLYMPUS i-SPEED monochrome camera is used. To minimize the influence of the arc, the camera is fitted with a band-pass filter with 20-nm bandwidth centered at a wavelength of 685 nm. In the experiment, frame rate, aperture, and shutter speed are some critical parameters to impact the quality of acquired reflected images, which may ultimately affect the accuracy of the measurement result.

System Configuration

In system configuration stage, some system parameters should be considered carefully. In addition to welding process-related parameters, such as welding current and speed, some important system position parameters are shown below.

Laser Position and Projection Angle

The position and angle of the laser diode determine the position/size of the projected pattern and the directions of incident lights. For the 19 × 19 dot-ma-

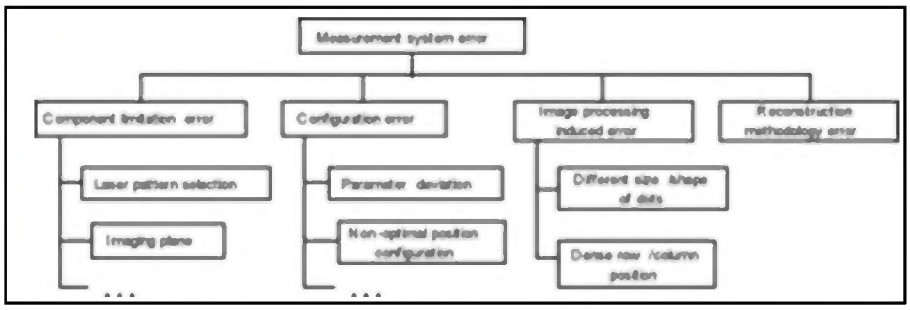

Fig. 5 — Classification of error sources.

trix pattern, the interbeam angle (0.77 deg) is used to present the angle between two adjacent projection rays (Ref. 16). In the system, the projected dot-matrix pattern on the workpiece should be big enough to cover the whole possible weld pool area (about 8 × 10 mm). The distance between the dots should be very small (less than 0.5 mm) in order to acquire detailed shape information.

The laser projection angle is defined as the angle between the center incident ray and workpiece. This parameter may affect the reflection of the laser lights. For example, for a slightly convex pool surface, if the angle is too large, the reflected lights may be blocked by the torch; if the angle is too small, some of the reflected lights will not be projected onto the imaging plane. Based on the experimental experiences, it is found that around 30 deg is proper for the laser projection angle.

Imaging Plane Position

The distance between the imaging plane and the torch (Z axis) directly impacts the size of reflected laser pattern and the arc intensity in the image. Experiments show the range of 45~60 mm is reasonable for the distance at a certain welding current range (65~75 A).

Image Processing

Figure 3A shows one of the acquired reflected images. As can be seen, only a part of projected dots in the 19 × 19 dot-matrix is reflected from the pool surface, and they are distorted as some convex curves. In the experiment, the projection angle of the laser diode is 31 deg and the distance between the laser diode and the origin of coordinate system (Fig. 2) is 31.5 mm. The distance between torch and imaging plane is 50 mm. The welding current is 75 A, and welding speed is 3 mm/s.

A point extracting algorithm and matching algorithm were developed to process the images (Ref. 14). First, the reflected points are extracted by using some image processing techniques, such as block threshold segmentation method, median filter, and morphological operations (Refs. 17, 18). Due to the dispersion of laser light and interference of arc light, the shapes of dots are distorted, which may make their positions imprecise. Based on the positions of reflected dots, some image features can then be determined (Ref. 14), such as row and column positions in Fig. 3B (Ref. 16). To investigate the possible correspondence relationship between projected and reflected dots, correspondence simulation was conducted (Ref. 14). The corresponding projected dots under sequential relationship are shown in Fig. 3C (Ref. 16). The correspondence relationship investigated by simulation simplifies the processing, but unavoidably introduces some errors.

Surface Reconstruction

Based on the acquired information, the next step was to reconstruct the three-dimensional weld pool surface. To resolve this issue, two schemes, interpolation and extrapolation reconstruction schemes (IRS and ERS), have been proposed to find an optimally estimated three-dimensional surface (Ref. 16). In the proposed schemes, first, a 3-D pool surface is estimated using either interpolation or extrapolation method in an iterative process, and then a 2-D boundary model is derived to find the surface boundary. Figure 4 shows the 3-D weld pool surfaces reconstructed by IRS and ERS for the reflected image in Fig. 3A. The result of ERS is more reasonable since the rear part of weld pool is lower than the other parts, which meets the result of direct observation (Ref. 16).

Error Analysis

Figure 5 shows the classification of the possible error sources according to four design and measurement procedures in the system. Here measurement system error refers to the overall error of the reconstructed 3-D weld pool surface caused by the proposed system.

Component limitation error refers to the error caused by the selected components. It is measured as the achievable minimal error by using the selected components. As mentioned before, the density of the laser pattern is one of the critical influence factors for measurement accuracy. Due to the availability, a 19 × 19 dot-matrix pattern is selected rather than a denser pattern. Some other nonideal components, such as self-designed imaging plane, may also contribute to component limitation error. This type of errors can be reduced by increasing the precision of the used components.

Configuration error is introduced because of the imprecise or improper parameters used in the system. Some deviations must exist between the measured nominal values and the actual values of the system parameters. Thus, parameter deviation is an error source. Possible ways to reduce this error include improving the system calibration method and averaging the values from multiple measurements. Nonoptimal system position parameters may also cause errors. For instance, if the position or projection angle of the laser diode is not properly configured, the laser pattern fails to cover the whole weld pool, which may ultimately make the reconstructed surface inaccurate.

In the step of image processing, the reflected dots are extracted from the background based on the intensity difference. As can be seen in Fig. 3A, the shape and size of reflected dots vary. Thus, it is hard to extract the positions of the reflected dots precisely. Furthermore, since the reflected dot-matrix pattern is distorted with densely distributed dots, sometimes it is very difficult to decide the row and column positions of the reflected dots. Hence, mismatch of the projected and reflected dot may also happen. These are the main sources of the "image processing induced error."

In the surface reconstruction process, the reflection point on the pool surface cannot be precisely decided based on the reflection law since only incident ray and its one reflected dot are known. Thus, in the reconstruction schemes an iteration process is proposed to find the optimal estimation for the weld pool surface. The error introduced by the reconstruction schemes is defined as "reconstruction methodology error."

It can be seen that there are many error sources in the measurement system. Among them, some error sources are random and unpredictable, such as the parameter deviation and the imaging processing induced error, while some errors are measurable and can be analyzed quantitatively through either experiments or simulations.

Measurement System Error

Measurement system error is the over-

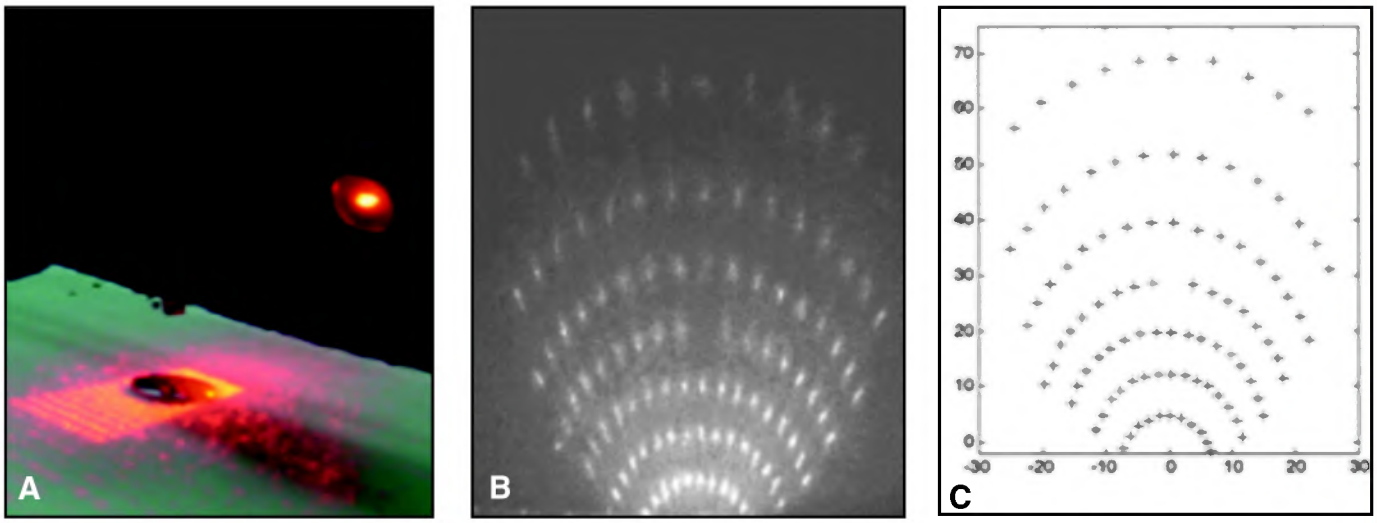

Fig. 6 — Experiment of measurement system error. A — Experiment design; B — captured image; C — extracted reflected dots on imaging plane.

all error of the measured 3-D weld pool surface. During the welding process, it is impossible to obtain the actual shape of the weld pool surface to compare with the measurement result. Thus, in order to estimate the overall measurement system error quantitatively, a thumb tack is selected to replace the weld pool for the experiment because the size and shape of its cap are similar to the weld pool, and its surface can reflect the laser light well. Figure 6A and B show the designed system and the acquired reflected image. In the experiment, the projection angle of the laser diode is 30.6 deg, and the distance between laser diode and origin of coordinate system is 46.4 mm. The distance between imaging plane and the torch is 40.7 mm. Figure 6C shows the result of image processing. The surfaces rebuilt by IRS and ERS are shown in Fig. 7. In the experiment, a circle model is used since the boundary shape of the thumb tack is known in advance. It can be seen that the shape of reconstructed surfaces fit the thumb tack well.

The reconstruction results from using the proposed 3-D measurement system can thus be compared with the thumb tack. Here the difference (error) in three dimensions can be calculated as the estimated measurement system error. Here the measurement error (E_{me}) can be defined as Equation 1.

$$E_{me} = \frac{|L_c - L_a|}{L_a} \cdot 100\% \quad (1)$$

where L_c presents the calculated value (of diameter or height) and L_a presents the actual value (of diameter or height). In the experiment, the diameter of the thumb tack is 9.75 mm, and its height is 0.91 mm. The diameters of the reconstructed pool boundaries in Fig. 7 are both 9.9 mm with

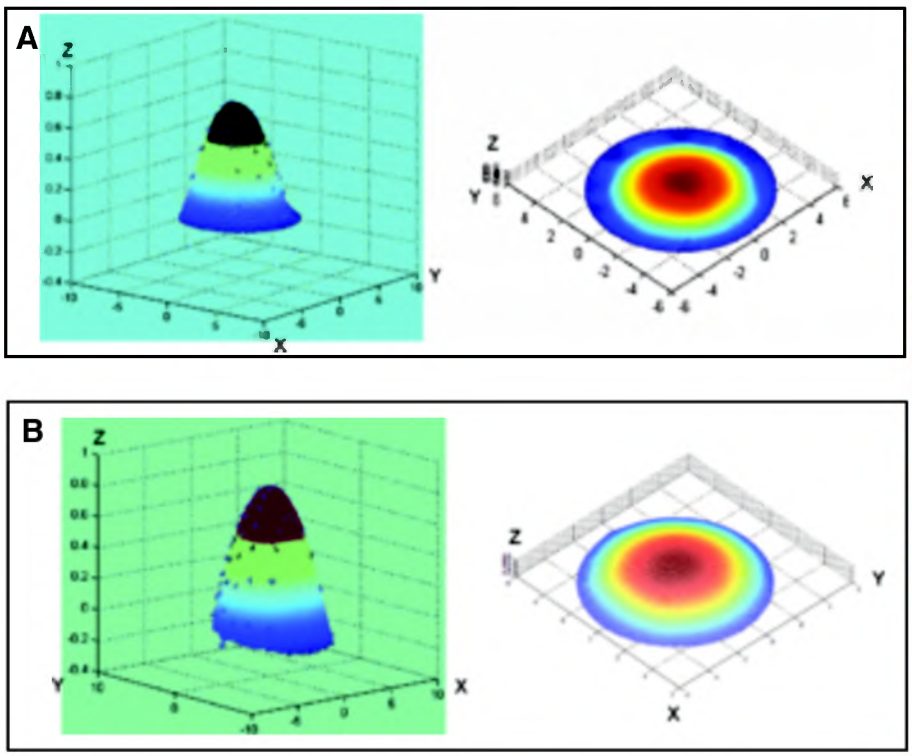

Fig. 7 — Reconstructed surfaces of the thumb tack. A — Result of IRS (view with magnified Z-axis and view with equal axes); B — result of ERS (view with magnified Z-axis and view with equal axes).

1.49% measurement system error. For IRS, the height of the pool surface is 0.75 mm with 17.8% measurement system error. For ERS, the calculated height of the surface (above Z=0 plane) is 0.83 mm with 9.1% measurement system error. It is obvious that the result of ERS is better than that of IRS. Since it is a measurement system for a small object, the achieved small measurement errors are acceptable.

Other Separated Errors

In this section, simulations are conducted to study some separated errors in the measurement system. In the error numerical simulation, first, the dot-matrix laser pattern is assumed to be projected onto some known surfaces. Thus, the corresponding reflected image on the imaging plane can be computed. Then the

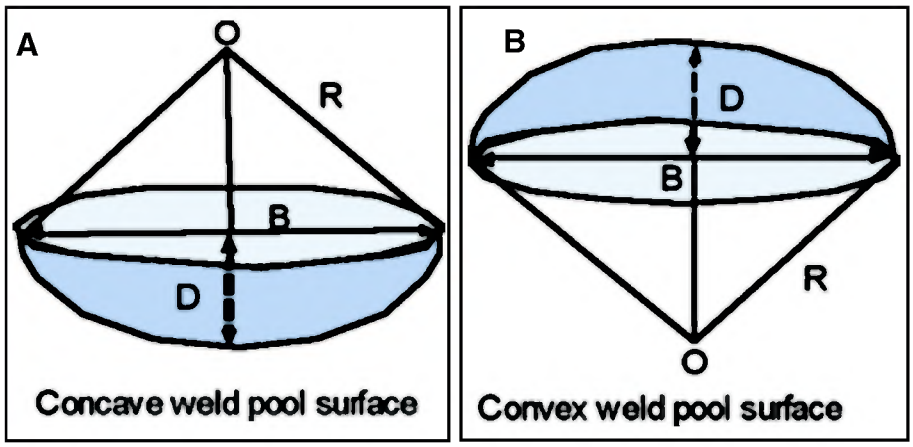

Fig. 8 — Two kinds of test surfaces. A — Concave simulation surface; B — convex simulation surface.

obtained reflected image is regarded as the captured images in the practical experiment and used to rebuild the pool surface. At last, the reconstructed result is compared with the known surface, thus the measurement error can be calculated.

Figure 8 shows the simplified concave and convex weld pool surfaces for simulation. The surfaces are a part of a sphere. In the figures, B refers to the diameter of the surface boundary (circle) and D is its depth. For the tested surfaces, the diameter B varies from 5 to 8 mm and the depth D changes from B/20 to B/10. These sizes are selected according to the practical dimensions of GTA weld pool surfaces.

Here three important errors are evaluated. They are configuration error, component limitation error, and reconstruction methodology error. Their corresponding main sources are nonoptimal configuration, nonideal laser pattern selection and iterative surface reconstruction scheme, respectively. Since these error sources are included in the sequential steps of measurement, these errors cannot be separated completely for error, measurement. Since all the errors should be calculated by using the same standard, we eliminate the error sources one by one and calculate the ultimate measurement errors of the reconstruction results in the designed three simulations. For simplicity reasons, the calculated measure errors are still called configuration error, component limitation error, and reconstruction methodology error. It will be seen later that these values are still reasonable estimates although the latter error(s) may be included in the former one.

Configuration Error

The configuration error is mainly caused by the nonoptimal displacement of the laser diode. In the simulation, only one case of nonoptimal displacement is studied as a representative to evaluate configuration error and the simulation parameters used are the same as the ones in the experiment discussed previously.

Dimensional Parameter Error

In order to describe the differences between the reconstructed and actual 3-D weld pool surfaces, two dimensional error measurement parameters are introduced: configuration error of depth (E_{ced}) and configuration error of boundary (E_{ceb}). They are defined as Equations 2 and 3, which are similar to the definition of measurement error.

$$E_{ced} = \frac{|D_c - D_a|}{D_a} \cdot 100\% \quad (2)$$

where D_c is the computed depth of the reconstructed surface and D_a is the actual depth of the simulated surface.

$$E_{ceb} = \frac{|B_c - B_a|}{B_a} \cdot 100\% \quad (3)$$

where B_c is the computed diameter of surface boundary, and B_a is the actual diameter of the simulated surface.

Figure 9 shows the configuration errors for different convex and concave surfaces by using the extrapolation reconstruction scheme (ERS). In the simulation, the boundary model has also been changed to a circle. As can be seen, E_{ceb} is very small for both convex and concave surfaces, and it is in a range of 0.03–2.51%, which shows the boundary model fits the tested surfaces well. But E_{ced} is relatively larger. For the convex surfaces, it varies from 0.78 to 10.85%. For the concave surfaces, it varies from 0.1 to 26.9%. The average of E_{ced} is about 8%.

It can be concluded that the error performance even under the same system configuration may vary greatly due to the different shapes/sizes of weld pool surfaces. For the large variation of E_{ced}, the possible explanation is in some cases laser dots are not projected onto the highest/lowest position of the convex/concave surfaces because of the limited density of the projected dot matrix (19 × 19). Thus, the height/depth of the surface cannot be reconstructed correctly by the reconstruction scheme. This phenomenon shows the optimal system configuration is only associated with a specific shape of weld pool surface, not all the situations.

Reflection Points Error

Despite the diameter and height/depth of the surface, the error caused by configuration can be further investigated by evaluating the differences of positions between computed and actual reflection point on the simulated weld pool surface. Since the tested surface is known, the difference can be achieved as average reflection point error E_{are} by using Equation 4.

$$E_{are} = \sum_{i,j} D_{i,j} / n, \ldots . (i,j) \in S \quad (4)$$

where S refers to the simulated surface and n represents the number of the reflection points on the surface. $D_{i,j}$ represents the distance between the computed reflection point $p'_{i,j}$ on the reconstructed surface and the actual reflection point $p_{i,j}$ on the tested surface. In the simulation, the average reflection error (E_{are}) by using ERS is in the range of (0, 0.25) mm. The small value of difference has verified the accuracy of the proposed reconstruction schemes.

It should be noted that the configuration error computed in Fig. 9 includes the component limitation error and reconstruction methodology error. Fortunately, as will be seen from the discussion below, these errors are very small. Hence, the above computation does give us a reasonable estimation of the configuration error.

Component Limitation Error

In order to minimize the impact of configuration parameters and investigate the component limitation error caused by 19 ×19 dot-matrix pattern, simulations with system position parameters in a reasonable range were conducted. The laser projection angle varied from 25 to 35 deg, and its distance to the origin of the coordinate system changed from 25 to 35 mm. Thus, the component limitation error can be estimated as the minimal error in the conducted simulations when the nominal optimal configuration is achieved.

Figure 10 shows the component limitation errors by applying ERS to different convex and concave surfaces. Here, two error parameters, called component limitation error of boundary (E_{leb}) and depth (E_{led}), are defined as similar to Equations 2 and 3. It can be seen in Fig. 10 the component limitation errors are much less

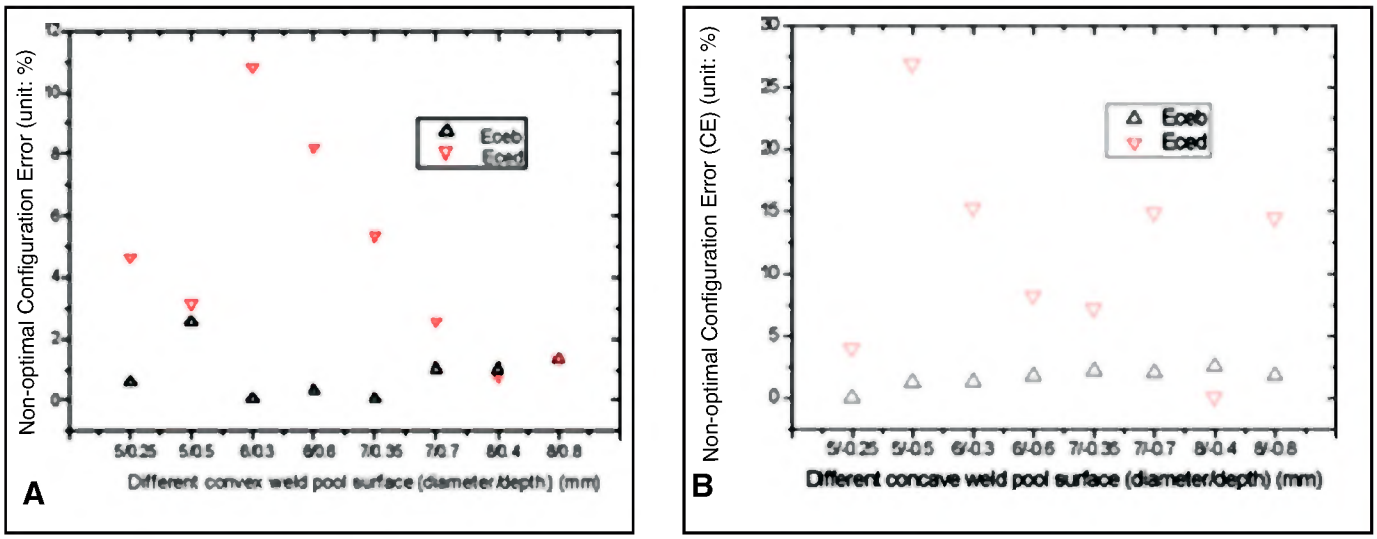

Fig. 9 — Configuration errors measured by using different surfaces. A — Convex surfaces; B — concave surfaces.

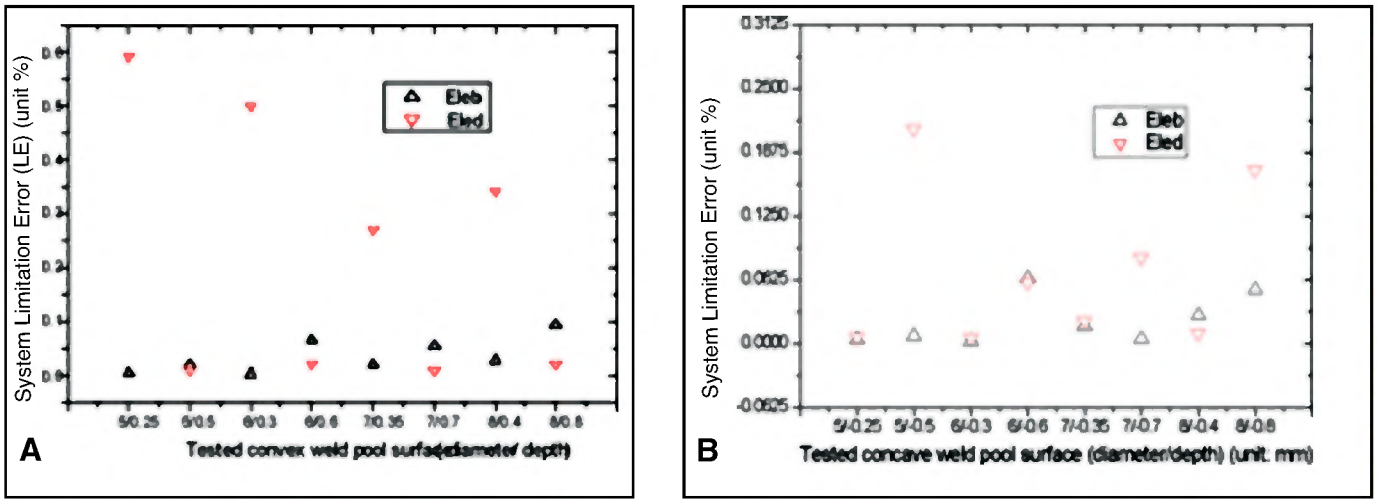

Fig. 10 — Component limitation error measured by using different surfaces. A — Convex surfaces; B — concave surfaces.

than the configuration errors in Fig. 9. In particular, the maximal boundary error is reduced from 2.8 to 0.1%, and the maximal depth error is reduced from 26.9 to 0.6%. Hence, the configuration error appears to be the major contributor to the overall measurement system error. Furthermore, the computed average reflection error (E_{are}) is less than 0.01 mm, which is much smaller than that in the configuration error simulation.

It is apparent that the computed system limitation error also includes the reconstruction methodology error. Hence, an investigation is needed to estimate the error caused by the reconstruction method.

Reconstruction Methodology Error

In the proposed measurement system, the reconstruction scheme itself may also introduce error because of some assumptions and approximations taken in it. Based on the simulation with various position configurations shown previously, a 39 ×39 dot-matrix pattern is used instead of a 19 ×19 dot-matrix pattern in order to evaluate the reconstruction methodology error with less impact of selected laser pattern. Although its scale is not approaching infinite by infinite, it is still reasonable to use it to estimate the error performance without the component limitation error. In the simulation, the interbeam angle of the dot-matrix laser pattern is decreased to 0.385 deg (half of its original value). Thus, the projected dots become denser and the projection area nearly stays unchanged.

Figure 11 shows the computed reconstruction methodology errors. Here reconstruction methodology error of boundary (E_{reb}) and depth (E_{red}) are also defined similar to Equations 2 and 3. Compared with the result of using 19 ×19 dot-matrix pattern, the calculated reconstruction methodology error by using 39 ×39 pattern is much less, and the values of E_{reb} and E_{red} are approaching to zero (maximum 0.17%) for both convex and concave surfaces. If given infinite dense projected dot-matrix, the reconstruction methodology error should not even exist. Of course, the small value of result is also related to the selected highly regulated simulation surfaces. The calculated average reflection error (E_{are}) is less than 0.005 mm, which is much smaller than that in the component limitation error simulation. It is evident that the insignificant reconstruction methodology error has proved the accuracy of the proposed reconstruction scheme.

Conclusion

Measurement of three-dimensional weld pool surface is an important and ur-

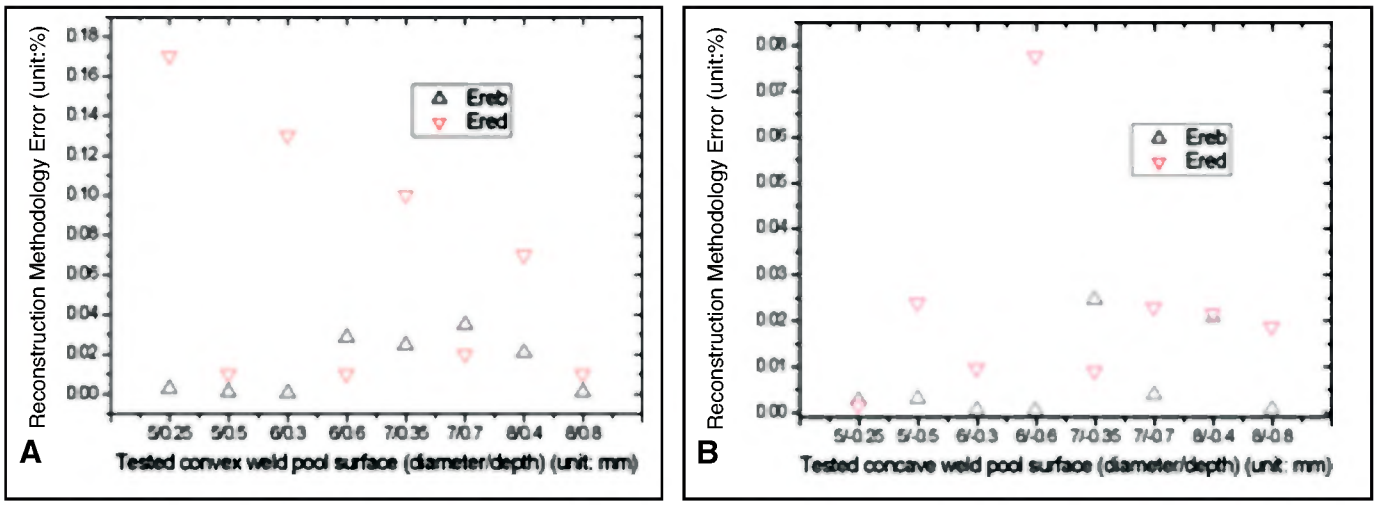

Fig. 11 — Reconstruction methodology errors measured by using different surfaces. A — Convex surfaces; B — concave surfaces.

gent task in the welding community. In our early work, a new 3-D measurement system has been proposed. Since the measured object is small and dynamic under harsh welding environment, an extensive error analysis of the measurement system is necessary.

In this paper, experiments and simulations have been conducted to evaluate various errors in the proposed 3-D measurement system. In the system, error sources have been divided into four types according to the measurement procedures. The authors found the following:

- The configuration error is the major error source that contributed to the overall measurement system error, whose average value is about 8%. Other studied errors, including the component limitation error (less than 1%) and surface reconstruction methodology error (less than 0.2%), are relatively insignificant.
- The configuration error is primarily caused by the mismatch of the projected laser pattern in relation to the particular weld pool surface to be measured. When the mismatch is eliminated, the configuration becomes optimal and the error reduces to the component limitation error. Reduction of the mismatch may be a method to improve the measurement accuracy significantly without changing either the components of the measurement system or the surface reconstruction method. In practical experiments, the variance of the weld pool surface makes it difficult to always achieve optimal configuration. Thus increase of the density of the projected laser dot-matrix appears to be a more practical and effective way to reduce both configuration error and component limitation error.
- Through the test for a physical object with known dimensions, the measurement system error was obtained (approximately 10% error by using ERS scheme). The reasonably small measurement error has verified the accuracy of the proposed three-dimensional specular surface measurement system.

Acknowledgment

This research is funded by the National Science Foundation under Grant DMI-0527889 — Sensors: Measurement of Dynamic Weld Pool Surface. H. Song also thanks the University of Kentucky Graduate School for the financial support through the Kentucky Opportunity Scholarship.

References

1. Groenwald, R. A., Mathieson, T. A., Kedzior, C. T., and Gaid, I. N. C. 1979. Acoustic emission weld monitor system — data acquisition and investigation. US Army Tank-Automotive Research and Development Command Report ADA085-518.

2. Siores, E. 1988. Development of a real-time ultrasonic sensing system for automated and robotic welding. PhD thesis. Brunel University.

3. Guu, A. C., and Rokhlin, S. 1989. Computerized radiographic weld penetration control with feedback on weld pool depression. *Mater. Eval.* 47: 1204–10.

4. Saeed, G. M. 2005. Three dimensional measurement of specular surfaces and its application in welding process. PhD thesis. University of Kentucky.

5. Kovacevic, R., Zhang, Y. M., and Ruan, S. 1995. Sensing and control of weld pool geometry for automated GTA welding. ASME *Journal of Engineering for Industry* 117(2): 210–222.

6. Kovacevic, R., and Zhang, Y. M. 1997. Real-time image processing for monitoring of free weld pool surface. *ASME Journal of Manufacturing Science and Engineering* 119(2): 161–169.

7. Mnich, C., Al-Bayat, F., Debrunner, C., Steele, J., and Vincent, T. 2004. In situ weld pool measurement using stereovision. *ASME, Proceedings Japan — USA Symposium on Flexible Automation*.

8. Choong, D. Y., and Jihye, L. 3D measurement of weld pool using biprism stereo vision sensor. *http://joining1.kaist.ac.kr/research/vision.htm*, Seoul National University.

9. Zhang, G., Yan, Z., and Wu, L. 2006. Reconstructing a three-dimensional P-GMAW weld pool shape from a two-dimensional visual image. *Measurement Science & Technology* 17: 1877–1882.

10. Zhao, D. 2000. Dynamic intelligent control for weld pool shape during pulsed GTAW with wire filler based on three-dimension visual sensing. Doctor thesis. Harbin Institute of Technology.

11. Li, L. 2005. Research on modeling of surface reflectance map and height calculation of pulse GTAW molten pool. Doctor thesis. Shanghai Jiao Tong University.

12. Du, Q. 2006. Extraction and intelligent control of 3D dynamic weld pool shape information of pulsed GTAW with wire filler. Doctor thesis. Shanghai Jiao Tong University.

13. Zhang, Y. M., Song, H. S., and Saeed, G. 2006. Observation of a dynamic specular weld pool surface. *Measurement Science & Technology* 17(6): L9–L12.

14. Song, H. S., and Zhang, Y. M. 2007. Image processing for measurement of three-dimensional GTA weld pool surface. *Welding Journal* 86: 323-s to 330-s.

15. Song, H. S., and Zhang, Y. M. 2007. Three-dimensional reconstruction of specular surface for gas tungsten arc weld pool. *Measurement Science & Technology* 18: 3751–3767.

16. Song, H. S., and Zhang, Y. M. 2008. Measurement and analysis of three-dimensional specular gas tungsten arc weld pool surface. *Welding Journal* 87(4): 85-s to 95-s.

17. Snyder, W. E., and Qi, H. 2004. *Machine Vision*. Cambridge University Press. ISBN 052183046X.

18. Gonzalez, R. C., and Woods, R. E. 2002. *Digital Image Processing*. Second edition. Prentice Hall.